International Endodontic Journal

doi:10.1111/j.1365-2591.2011.01864.x

The influence of carbon content on cyclic fatigue of NiTi SMA wires

T. C. U. Matheus[1,2], W. M. M. Menezes[1], O. D. Rigo[1], L. K. Kabayama[1], C. S. C. Viana[2,3] & J. Otubo[1]

[1]Instituto Tecnologico de Aeronautica-ITA, Sao Paulo; [2]Instituto Militar de Engenharia-IME, Rio de Janeiro; and [3]Universidade Federal Fluminense-UFF, Rio de Janeiro, Brazil

Abstract

Matheus TCU, Menezes WMM, Rigo OD, Kabayama LK, Viana CSC, Otubo J. The influence of carbon content on cyclic fatigue of NiTi SMA wires. *International Endodontic Journal*, **44**, 567–573, 2011.

Aim To evaluate two NiTi wires with different carbon and oxygen contents in terms of mechanical resistance to rotary bending fatigue (RBF) under varied parameters of strain amplitude and rotational speed.

Methodology The wires produced from two vacuum induction melting (VIM) processed NiTi ingots were tested, Ti-49.81at%Ni and Ti-50.33at%Ni, named VIM 1 and VIM 2. A brief analysis related to wire fabrication is also presented, as well as chemical and microstructural analysis by energy dispersive spectroscopy (EDS) and optical microscope, respectively. A computer controlled RBF machine was specially constructed for the tests. Three radii of curvature were used: 50.0, 62.5 and 75.0 mm, respectively, R_1, R_2 and R_3, resulting in three strain amplitudes ε_a: 1.00%, 0.80% and 0.67%. The selected rotational speeds were 250 and 455 rpm.

Results The VIM 1 wire had a high carbon content of 0.188 wt% and a low oxygen content of 0.036 wt%. The oxygen and carbon contents of wire VIM 2 did not exceed their maximum, of 0.070 and 0.050 wt%, according to ASTM standard (ASTM F-2063-00 2001). The wire with lower carbon content performed better when compared to the one with higher carbon content, withstanding 29 441 and 12 895 cycles, respectively, to fracture.

Conclusions The surface quality of the wire was associated with resistance to cyclic fatigue. Surface defects acted as stress concentrators points. Overall, the number of cycles to failure was higher for VIM 2 wires with lower carbon content.

Keywords: carbon contents, NiTi SMA wires, rotary bending fatigue tests.

Received 18 December 2009; accepted 3 January 2011

Introduction

NiTi (nickel–titanium) alloys are one of the best shape memory alloys (SMA), with applications in the aerospace industry, in robotics and medicine and dentistry. In dentistry, the major uses are in orthodontics and endodontics, and the property of superelasticity is essential for these applications (Bahia *et al.* 2005).

Correspondence: T. C. U. Matheus, Instituto Tecnologico de Aeronautica. Praça Marechal Eduardo Gomes, 50, Vila das Acacias, CEP: 12228-900, Sao Jose dos Campos, Sao Paulo, Brazil (Tel.: +55 12 39475905; fax: +55 12 39475906; e-mail: tcmatheus@yahoo.com.br).

Scientific and technological progress has allowed improvements in endodontic instruments, mainly in terms of mechanical properties. It is possible to produce endodontic files machined from superelastic NiTi SMA that allows rapid and effective biomechanical preparation of the root canal. However, a major concern when using NiTi rotary instruments is the possibility of unexpected failure because of flexural fatigue during the rotation of an instrument in a curved root canal. Usually, the file does not exhibit a visible indication that the failure will occur, especially when it is misused (Sattapan *et al.* 2000, Lopes *et al.* 2001).

For NiTi SMA wires, the fatigue loading could be influenced by factors such as surface defects and precipitates that may act as stress concentrators.

Through chemical and microstructural characterization of superelastic NiTi alloys, it is possible to detect the presence of TiC particles from carbon contamination during the melting stage of the production process. Usually NiTi SMA are produced by vacuum induction melting (VIM) using a graphite crucible that contaminates the bath with carbon, and the degree of contamination depends upon the crucible quality. Consequently, the wire produced by these materials will also contain different amounts of carbon content and therefore different amounts of TiC particles, thus influencing the resistance of the wire to rotary bending fatigue (RBF) tests (Matheus *et al.* 2007, Menezes *et al.* 2008).

The RBF tests have emerged as a standard test for the structural fatigue test of shape memory wires used in endodontic applications. Fatigue rupture life decreased as wire diameters increased from 1.0 to 1.4 mm, and reduced rupture life was observed as rotational speeds were increased from 100 to 800 rotations per min (rpm) (Wagner *et al.* 2004). According to the literature (Sawaguchi *et al.* 2003), fatigue life decreases as the strain amplitude increases.

When considering the application of NiTi wire to produce endodontic files, several NiTi wires were produced and tested at the Instituto Tecnologico de Aeronautica-ITA using RBF tests to evaluate cyclic fatigue resistance, varying parameters such as carbon and oxygen contents, radius of curvature of the wire and rotational speed. In this study, an apparatus for the RBF test is described.

Materials and methods

Two VIM processed NiTi ingots were tested, Ti-49.81at%Ni and Ti-50.33at%Ni with different carbon and oxygen contents, hereafter named VIM 1 and VIM 2. These materials had their chemical composition of matrix and impurities determined through the X-ray fluorescence spectroscopy (XRFS). The ingots were then hot forged and cold drawn down to 1.0 mm in diameter wire. The cold drawing was achieved with a 15% area reduction per pass with intermediate annealing at 500 °C for 10 min. The cold drawn wire was heat treated and straightened (memorized) in a tube furnace at 400 °C under an axial stress of 125 MPa.

Microstructural analysis was carried out after wire drawing, and the TiC particle distribution was evaluated in an ‘as polished’ condition using an optical microscope and scanning electron microscopy (SEM). The presence of TiC particles was determined by energy dispersive spectroscopy (EDS) (Gall *et al.* 2001). The wire surface and fracture surface after the RBF tests were evaluated through SEM analysis.

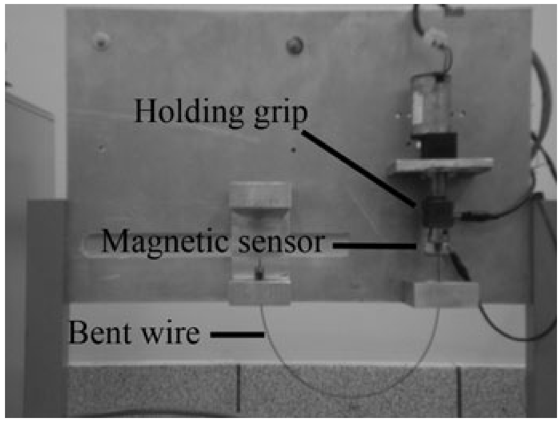

Figure 1 NiTi wire mounted in rotary bending fatigue device, test control by microcomputer.

A RBF device (Sawaguchi *et al.* 2003, Wagner *et al.* 2004, Patel 2005, Figueiredo *et al.* 2006) is shown in Fig. 1, indicating the bent wire forced in rotation by the holding grip connected to a driving motor. A low-friction nylon® bearing lubricated with MoS_2 grease was used to minimize torsional friction of the wire. The number of cycles, the rotational speed and the time to failure of the wire were automatically controlled by a computer. The number of cycles until the wire failure was recorded by a magnetic sensor.

Three radii of curvature of the wires were used: 50.0, 62.5 and 75.0 mm, respectively, denoted as R_1, R_2 and R_3, resulting in three strain amplitudes ε_a of 1.00, 0.80% and 0.67%. The selected rotational speeds were 250 and 455 rpm (Sawaguchi *et al.* 2003, Wagner *et al.* 2004). Three samples with 1.0-mm-diameter wire were tested for each condition of radius of curvature and rotational speed of the wire. The tests were carried out at room temperature kept at 20 °C.

Results

The chemical compositions of the wires are shown in Table 1. The wire VIM 2 is a nickel-rich alloy, with its

Table 1 Nickel, carbon and oxygen content in the vacuum induction melting (VIM) 1 and VIM 2 alloys

	Ni (at%)	C (wt%)	O (wt%)
VIM 1	49.81	0.188	0.036
VIM 2	50.33	0.052	0.057
ASTM F-2063-00 2001	–	0.050 max	0.070 max

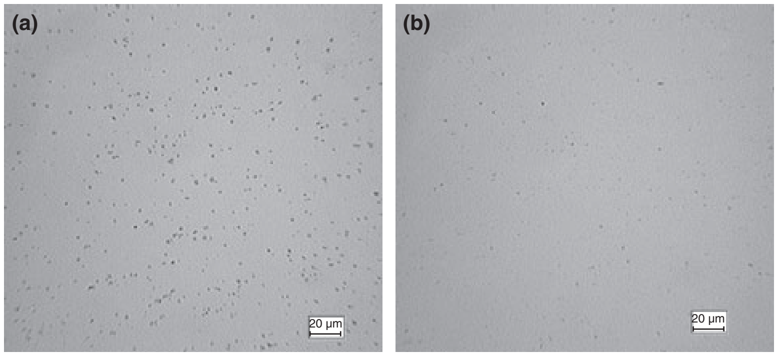

Figure 2 Metallographics samples vacuum induction melting (VIM) 1 (a) and VIM 2 (b) with 1.37 mm diameter, with no acid etching.

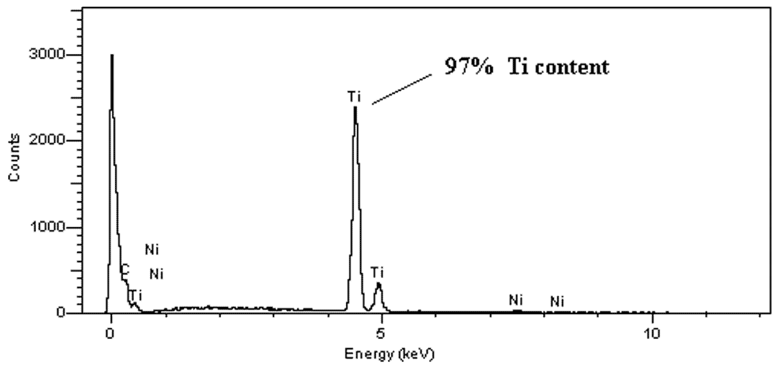

Figure 3 Energy dispersive spectroscopy analysis on the precipitates.

oxygen and carbon contents not exceeding a maximum of 0.070 and 0.050 wt%, according to ASTM standard (ASTM F-2063-00 2001). The wire VIM 1 had a high carbon content of 0.188 wt%, therefore well above the established limit and a low oxygen content of 0.036 wt%. As a result (Fig. 2), the VIM 1 alloy had a high density of TiC precipitates compared to the VIM 2 alloy, as predicted by chemical analysis (Table 1). The EDS analysis on the precipitates indicated high Ti content (approximately 97%; Fig. 3), which is in agreement with data reported elsewhere (Gall *et al.* 2001).

The RBF test results when varying strain amplitude (ε) and rotational speed (ω) are shown in Tables 2 and 3. Starting with ω = 250 rpm for VIM 1, the number of cycles, N_f, increased as the strain amplitude decreased; the maximum individual value was 108 323 cycles. Except for the last datum, the average performance of VIM 2 was marginally better than that of VIM 1. The influence of increase in rotational speed, lowering the average N_f values for both wires, can be seen in Table 3. Again, except for the last datum for ε_a = 0.67%, the better performance of VIM 2 is also demonstrated. Figs 4 and 5 summarize the N_f values for both wires as a function of strain amplitude and rotational speed.

Table 2 Rotary bending fatigue tests results for the rotational speed of 250 rpm

Curvature radius/strain amplitude	250 rpm			
	VIM 1		VIM 2	
	N_f	Average	N_f	Average
50 mm 1.00%	21 014	29 815	43 835	38 301
	34 903		48 285	
	33 529		22 785	
62.5 mm 0.80%	17 779	30 171	28 281	31 380
	36 385		41 714	
	36 351		24 147	
75 mm 0.67%	61 441	68 754	52 571	39 497
	36 500		40 856	
	10 8323		25 336	

VIM, vacuum induction melting.

Figure 6 demonstrates that the wire surfaces for both VIM 1 and VIM 2 are smooth without defects, and these wires withstood a significantly larger number of cycles before failure. The VIM 1 wire withstood more than 100 000 cycles at the lowest strain amplitude and lowest rotational speed. At the highest

Table 3 Rotary bending fatigue tests results for the rotational speed of 455 rpm

Curvature radius/strain amplitude	455 rpm			
	VIM 1		VIM 2	
	N_f	Average	N_f	Average
50 mm 1.00%	10 339	12 895	24 855	29 441
	14 028		29 694	
	14 320		33 775	
62.5 mm 0.80%	7229	9057	35 323	29 127
	11 580		25 665	
	8362		26 395	
75 mm 0.67%	50 203	41 733	39 363	37 570
	37 911		34 955	
	37 087		38 394	

VIM, vacuum induction melting.

strain amplitude of 1.00% but with the same rotational speed, the result presented by VIM 2 was 48 285 cycles at failure.

The worst result was presented by VIM 1 with N_f = 7229 cycles, showing a very large longitudinal

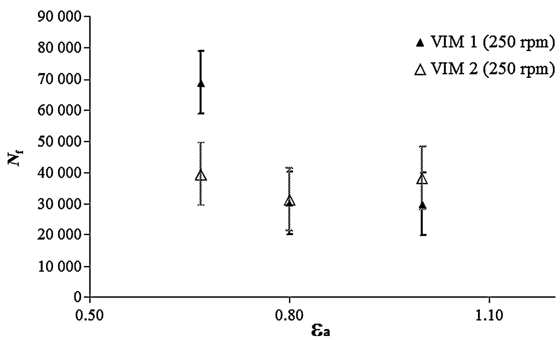

Figure 4 Average N_f values as a function of strain amplitude and rotational speed, ω = 250 rpm.

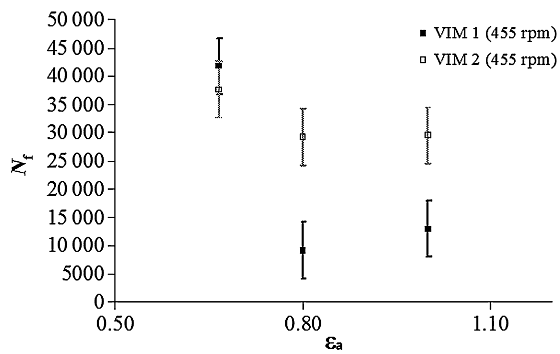

Figure 5 Average N_f values as a function of strain amplitude and rotational speed, ω = 455 rpm.

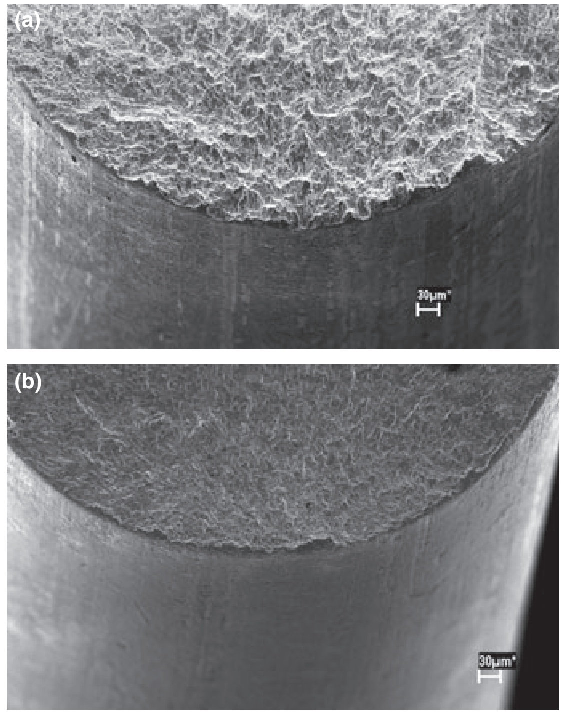

Figure 6 Wire surfaces with no defects: (a) vacuum induction melting (VIM) 1, ε_a = 0.67%, ω = 250 rpm, N_f = 108 323 and (b) VIM 2, ε_a = 1.00%, ω= 250 rpm, N_f = 48 285 (b), scanning electron microscopy.

crack nucleated at the fracture (Fig. 7a). For VIM 2, the worst result was 24 147 cycles with intermediate strain amplitude and lower rotational speed, and fracture was nucleated at a fold-like defect, as can be clearly seen in Fig. 7(b). The lightest condition (lower strain amplitude and lower rotational speed) with the worst result for wire VIM 2 is shown in Fig. 8, showing a scratch-like defect (promoted by the wire drawing stage), presenting breakage with 25 336 cycles.

Discussion

It must be highlighted that the superelastic shape memory wires used in this study exhibited a unique property and could be bent into a semicircular shape (with a radius as small as 50 mm) and forced into rotation for many cycles before they failed. The RBF rupture data reported in this study are in good qualitative agreement with previously published results (Sawaguchi *et al.* 2003).

In relation to the chemical compositions of the wires, the nickel content of wire VIM 1 is about 0.52%

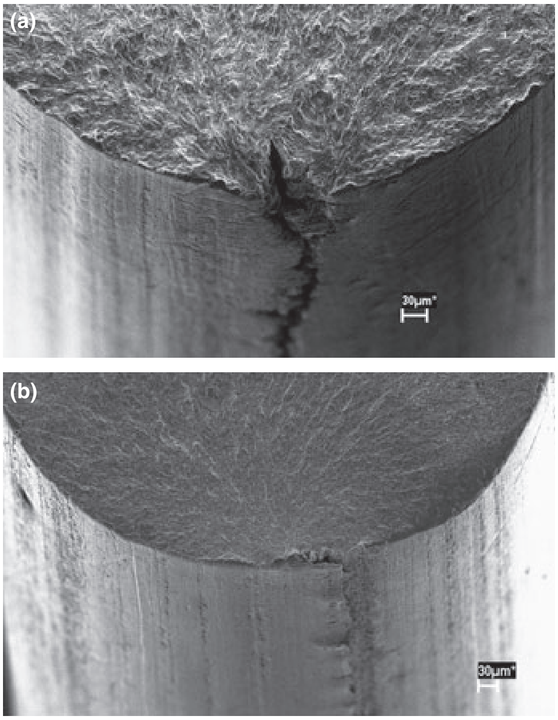

Figure 7 Wire and fractures surfaces of: (a) vacuum induction melting (VIM) 1 ε_a = 0.80%, ω = 455 rpm, N_f = 7229 with longitudinal cracks and (b) VIM 2, ε_a = 0.80%, ω = 250 rpm, N_f = 24 147 with folding-like irregularities, scanning electron microscopy.

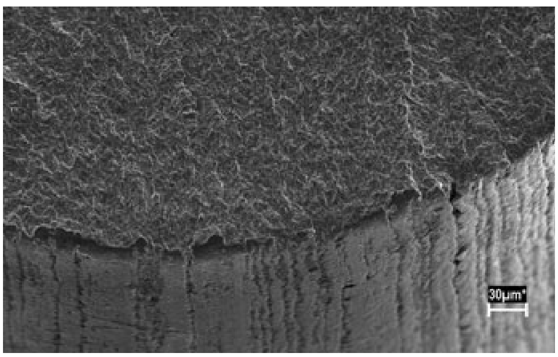

Figure 8 Vacuum induction melting 2 wire and fracture surfaces, ε_a = 0.67%, ω = 250 rpm, N_f = 25 336 cycles with scratch like defects, scanning electron microscopy.

Table 4 Transformations temperatures, in °C

	M_S	M_P	M_F	A_S	A_P	A_F
VIM 1	−9.5	−18	−27.5	−5.6	4.1	12.9
VIM 2	2.8	−4.9	−16.2	6	17	27.2

M_S martensite start, M_P martensite peak, M_F martensite finish, A_S austenite start, A_P austenite peak, A_F austenite finish; VIM, vacuum induction melting.

lower than that of VIM 2. According to the nickel content, wire VIM 1 should present a higher martensitic transformation temperature compared to wire VIM 2; however, as shown in Table 4, their martensitic transformation temperatures are almost the same (Otubo *et al.* 2008). As shown in Table 4, both wires are superelastic at room temperature. This result comes from the very high carbon content of VIM 1, 0.188 wt%, which is 3.6 times higher than that of VIM 2, 0.052 wt%. As shown in an earlier work, the presence of carbon, besides interfering in mechanical performance, modifies the martensitic transformation temperature. Carbon reacts with titanium forming TiC to modify the Ni/Ti relation and transform the matrix to be richer in nickel, therefore, lowering the martensitic transformation temperature (Otubo *et al.* 2008).

The influence of mechanical parameters (strain amplitude and rotational speed) was smaller for VIM 2 than for VIM 1, but for both alloys, the N_f values decreased with increasing strain amplitude and rotational speed (Tobushi *et al.* 1997, Sawaguchi *et al.* 2003, Patel 2005). Also, there was a significant effect of wire diameter on fatigue rupture life, thicker wires fractured earlier than thin wires and higher rotational speeds were associated with lower rupture lives (Sawaguchi *et al.* 2003). According to Fig. 4, the influence of strain amplitude was stronger for VIM 1 than for VIM 2. This behaviour can also be observed in Fig. 5. On average, the alloy VIM 2 was more fatigue-resistant than the alloy VIM 1, showing the positive influence of the low carbon content for increasing the fatigue life. However, for the strain amplitude of 0.67%, the results were better for VIM 1 wires than for VIM 2, at 250 rpm and at 455 rpm, and these results should be associated with the surface quality of the wires. The large data scatter seen in Tables 2 and 3 is attributed to the surface quality of the wires, as seen before. It was expected that the VIM 2 wire should present better performance than VIM 1, which did not occur. Corroborating with the above statement, the best results for both wires VIM 1 and VIM 2 were found in the wires with no surface defects as they withstood a significantly larger number of cycles before failure, as expected. According to the literature (Sawaguchi *et al.* 2003, Prymak *et al.*

2004), the fracture initiation processes are dependent on the presence of defects such as cracks, scratches, folds and extrusion-like surface irregularities, which can be associated with large data scatter in N_f. Similarly, for endodontic instruments, the sources of cracks were usually found at the cutting edge or radial land region, which are the stress concentrator points owing to machining defects. This is to be expected because when a circular wire is bent, its crystallographic orientation in the outside region is subjected to the greatest stress and strain. Indeed, the first fatigue crack often is initiated at the surface (Cheung & Darvell 2007).

Taking into account the carbon content, the VIM 1 wire should have had a less satisfactory performance when compared to VIM 2, but this behaviour was sometimes influenced by the surface quality, as shown in the results of this work. Therefore, to enhance the effect of carbon content on the performance in RBF tests, the quality of the wire surface should be improved. In that way, it is possible to separate the effect of surface quality from the influence of carbon and oxygen contamination on the performance of the wire in RBF test. As a consequence, the better understanding of those effects will contribute to the definition of raw material for the production of improved endodontic instruments.

Conclusions

NiTi wire production is feasible, and the test apparatus could be used for RBF tests. On average, the number of cycles to failure was higher for VIM 2 wires with a lower carbon content, as expected. However, the best result was found in the defect-free VIM 1 wire with more than 100 000 cycles before wire fracture. The worst result occurred with the VIM 1 wire with 7229 cycles to failure owing to a large longitudinal crack. Thus, the presence of surface defects associated with mechanical processing plays an important role for RBF resistance, masking the effect of carbon content. The quality of the wire should be improved to better understand the real effect of carbon on RBF performance.

Acknowledgements

We thank FAPERJ (grant #E-26/100.130/06-DSC 10) for scholarship to one of the authors; FAPESP (grant #00/09730-1); FINEP (grant # 01.04.0255.00 – CT INFRA 03/2003; PROINFRA 01/05, Protocol 153) for financial support; and FATEC-EXPOENTE for supporting the BRF device construction.

References

ASTM F-2063-00 (2001) Standard Specification for wrought nickel-titanium shape memory alloys for medical devices and surgical implants. Copyright ASTM International - American Society for Testing and Materials.

Bahia MGA, Martins RC, Gonzalez BM, Buono VTL (2005) Physical and mechanical characterization and the influence of cyclic loading on the behavior of nickel-titanium wires employed in the manufacture of rotary endodontic instruments. *International Endodontic Journal* **38**, 795–801.

Cheung GSP, Darvell BW (2007) Fatigue testing of a NiTi rotary instrument. Part 1: strain-life relationship. *International Endodontic Journal* **40**, 612–8.

Figueiredo AMG, Mondenesi PJ, Buono VTL (2006) Caracterizacao de fadiga de ligas superelasticas de NiTi em ensaios de flexao rotativa. In: *Proceedings of the 61st Annual Congress of Brazilian Association of Metallurgy*. Rio de Janeiro, RJ, Brazil: Brazilian Association of Metallurgy, pp. 50–4.

Gall K, Yang N, Sehitoglu H, Chumlyakov YI (2001) Fracture of precipitated NiTi shape memory alloy. *International Journal of Fracture* **109**, 189–207.

Lopes HP, Elias CN, Siqueira Junior JF, Araujo Filho WR (2001) Fratura por torcao de limas endodonticas de aco inoxidavel e niquel-titanio. *Revista Paulista de Odontologia* **23**, 8–12.

Matheus TCU, Menezes WMM, Rigo OD *et al.* (2007) NiTi SMA wires subjected to rotary bending fatigue tests. In: *Proceedings of The International Conference on Shape Memory and Superelastic Technologies – SMST*. Tsukuba, Japan: Shape Memory and Superelastic Technologies – SMST, pp. 239–46.

Menezes WMM, Matheus TCU, Kabayama LK, Rigo OD, Otubo J (2008) Efeito da presenca de carbonetos de titanio sobre a vida em fadiga por flexao rotativa da liga NiTi com efeito memoria de forma. In: *Proceedings of the 63rd Annual Congress of Brazilian Association of Metallurgy*. Santos, S. Paulo, Brazil: Brazilian Association of Metallurgy, pp. 1327–37.

Otubo J, Rigo OD, Coelho AA, Neto CM, Mei PR (2008) The influence of carbon and oxygen content on the martensitic transformation temperatures and enthalpies of NiTi shape memory alloys. *Materials Science and Engineering: A* **481–482**, 639–42.

Patel MM (2005) Characterizing fatigue and fracture response of medical grade nickel-titanium alloys by rotary beam testing. http://www.fwmetals.com/resources_whitepapers 1–12.

Prymak O, Klocke A, Kahl-Nieke B, Epple M (2004) Fatigue of orthodontic nickel-titanium (NiTi) wires in different fluids under constant mechanical stress. *Materials Science and Engineering: A* **378**, 110–4.

Sattapan B, Nervo GJ, Palamara JEA, Messer HH (2000) Defects in rotary nickel-titanium files after clinical use. *Journal of Endodontics* **26**, 161–5.

Sawaguchi T, Kausträter G, Yawny A, Wagner M, Eggeler G (2003) Crack initiation and propagation in 50.9 at Pct NiTi pseudoelastic shape memory wires in bending-rotation fatigue. *Metallurgical and Materials Transactions A* **34**, 2847–60.

Tobushi H, Hashisuka T, Yamada S, Lin PH (1997) Rotating-bending fatigue of a NiTi shape-memory alloy wire. *Mechanics of Materials* **26**, 35–42.

Wagner M, Sawaguchi T, Kausträter G, Höffken D, Eggeler G (2004) Structural fatigue of pseudoelastic NiTi shape memory wires. *Materials Science and Engineering: A* **378**, 105–9.